

RemoteTrimmer: Adaptive Structural Pruning for Remote Sensing Image Classification

1st Guangwenjie Zou
Hohai University
Nanjing, China
guangwenjiezou@hhu.edu.cn

1st Liang Yao
Hohai University
Nanjing, China
liangyao@hhu.edu.cn

3rd Fan Liu
Hohai University
Nanjing, China
fanliu@hhu.edu.cn

4th Chuanyi Zhang
Hohai University
Nanjing, China
zhangchuanyi@hhu.edu.cn

5th Xin Li
Hohai University
Nanjing, China
li-xin@hhu.edu.cn

6th Ning Chen
Hohai University
Nanjing, China
cn@hhu.edu.cn

7th Shengxiang Xu
Hohai University
Nanjing, China
xushx@hhu.edu.cn

8th Jun Zhou
Griffith University
South East Queensland, Australia
jun.zhou@griffith.edu.au

Abstract—Since high resolution remote sensing image classification often requires a relatively high computation complexity, lightweight models tend to be practical and efficient. Model pruning is an effective method for model compression. However, existing methods rarely take into account the specificity of remote sensing images, resulting in significant accuracy loss after pruning. To this end, we propose an effective structural pruning approach for remote sensing image classification. Specifically, a pruning strategy that amplifies the differences in channel importance of the model is introduced. Then an adaptive mining loss function is designed for the fine-tuning process of the pruned model. Finally, we conducted experiments on two remote sensing classification datasets. The experimental results demonstrate that our method achieves minimal accuracy loss after compressing remote sensing classification models, achieving state-of-the-art (SoTA) performance.

Index Terms—Model Compression, Structural Pruning, Remote Sensing Image Classification, Adaptive Training.

I. INTRODUCTION

Remote sensing technology has attracted significant attention due to its ability to remotely capture diverse and extensive environmental data [1]–[5]. As one of the most significant techniques in remote sensing, image classification has been applied to agricultural crop monitoring, urban planning, and biodiversity assessment [6]–[9]. Despite its extensive applicability, Remote Sensing Image Classification (RSIC) still faces several challenges. For example, remote sensing images typically have high resolution. To ensure classification accuracy, mainstream approaches classify images by dividing

Guangwenjie Zou and Liang Yao contributed equally to this work. Corresponding author: Fan Liu.

This work was partially supported by the Fundamental Research Funds for the Central Universities (No. B240201077), National Nature Science Foundation of China (No. 62372155 and No. 62302149), Aeronautical Science Fund (No. 2022Z071108001), Joint Fund of Ministry of Education for Equipment Pre-research (No. 8091B022123), Water Science and Technology Project of Jiangsu Province under grant No. 2021063, Qinglan Project of Jiangsu Province, Changzhou science and technology project No. 20231313. The work of Liang Yao was supported in part by Postgraduate Research & Practice Innovation Program of Jiangsu Province (No. SJCX24_0183).

Our code is available at: <https://github.com/1e12Leon/RemoteTrimmer>.



(a) Comparison of Image Features between ImageNet (Left) and UCM (Right)



(b) Blurred Remote Sensing Image

Fig. 1. Motivations of our proposed method. (a) Comparison of general (ImageNet) and remote sensing (UCM) images. Remote sensing images have top-down views from different heights, resulting in greater scale variations of the objects. This situation usually leads to the narrowing of differences between similar object features. (b) Remote sensing images often suffer from unclear images with atmospheric noise pollution, which makes lightweight models learning more difficult.

them into smaller patches. However, this divide-and-conquer strategy exponentially increases inference time. Meanwhile, high-precision classification models typically involve numerous parameters, further escalating the model inference time. These challenges limit the efficiency and scalability of RSIC.

To accelerate inference speed, a common approach is to reduce redundant parameters through various model compression techniques, such as pruning [10], knowledge distillation [11], and model quantization [12]. Pruning, in particular, has attracted significant attention due to its ease of implementation on original models [13], [14]. As represented in Fig. 1 (a), compared to general domain images, remote sensing images have a top-down perspective and variations in object scale [15]–[17], which makes feature extraction more challenging. As a result, the differences in channel impor-

tance become less pronounced [15], [18], [19]. Therefore, although existing methods achieve remarkable compression performance in general domains [20]–[22], their performance in remote sensing tasks still has shortcomings.

Furthermore, some researchers adopt or develop lightweight models to enhance inference speed, such as literature [23] and RSCNet [24]. However, while effective in reducing computational costs, these models frequently struggle with limited capabilities in feature extraction and learning [25]–[28]. Therefore, the performance of such models may decline when faced with difficult samples in remote sensing domain. For example, as shown in Fig. 1 (b), the presence of blurred images caused by atmospheric noise is challenging for lightweight models to learn and classify. Prioritizing challenging samples is essential for maintaining the performance of lightweight models.

To this end, we introduce a novel model pruning method for remote sensing image classification, named **RemoteTrimmer**. It is composed of a Channel Attention Pruning (CAP) strategy and an Adaptive Mining Loss (AML). Specifically, we design CAP module to enhance channel importance differentiation by mapping the original model’s features into a channel attention space, contributing to more precise pruning. Next, we introduce the AML function to emphasize difficult samples during the fine-tuning of pruned models, improving overall performance. To validate the effectiveness of our approach, we conduct experiments on two remote sensing classification datasets with two different models. Extensive experiments demonstrate that our approach effectively reduces the model’s parameters, resulting in faster inference speed while preserving strong performance across two datasets.

Our main contributions are highlighted as follows:

- We propose a novel pruning method by amplifying the differences in importance of model channels. **To the best of our knowledge, this is the first pruning method for remote sensing image classification models.**
- We propose an adaptive mining loss function for the fine-tuning process of pruned lightweight models. It can adaptively learn difficult samples to reduce the accuracy loss caused by pruning.
- Our approach achieves state-of-the-art (SoTA) performance on the EuroSAT and UCMerced_LandUse datasets. The accuracy of the model after pruning can even be higher than before pruning.

II. METHOD

In this section, we introduce our proposed efficient structural pruning approach for remote sensing image classification, **RemoteTrimmer**. The overall framework is represented in 2.

A. Channel Attention Pruning

The significant scale variation of objects in remote sensing images, combined with the less distinct object features compared to general domains, results in reduced inter-channel differences within the model [15], [18]. The situation may adversely affect the performance of general pruning algorithms.

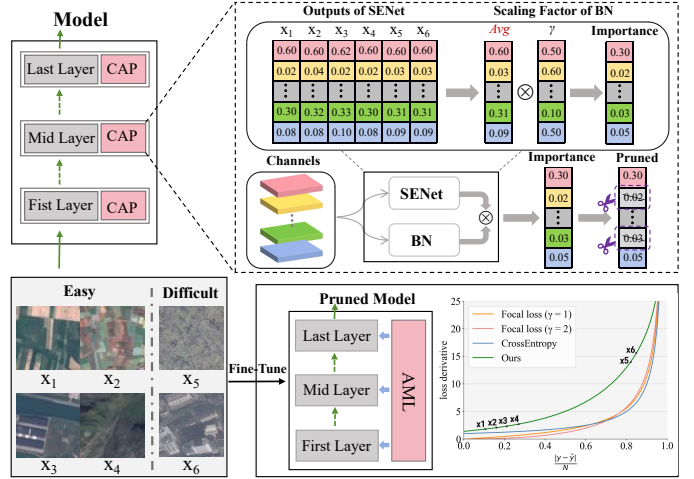


Fig. 2. Overview of our RemoteTrimmer. In the pruning phase, we leverage intermediate outputs from SENet and scaling factors from the BN layer to map channel importance into the attention space. During the post-pruning fine-tuning phase, we design a lateral inhibition loss function to emphasize difficult samples. Our method effectively addresses two key challenges in remote sensing model pruning: the lack of distinct channel importance and the prevalence of difficult samples.

Therefore, we propose to amplify the differences in channel importance by mapping the channel features to a new space.

Channel attention allows the model to dynamically adjust the importance of each channel [29]. Inspired by it, we incorporate a channel attention module into the pruning process, mapping channel features into a new attention space. In this space, the contribution of each channel is amplified, which helps in identifying and pruning less significant channels. Specifically, during the pruning phase, we leverage the intermediate output of Squeeze-and-Excitation Network (SENet) [30] to adjust the scaling factor γ in the atch Normalization (BN) layer. This adjustment enables γ to focus on the more important channels. Utilizing ResNet18 [31] as an example, the process involves the following steps:

First, we apply the SENet module to ResNet18 and train the network. Then, we extract the intermediate output of SENet. The intermediate output at the i -th convolutional layer of SENet can be expressed as follows:

$$s_i = \sigma(W_2 \cdot \text{ReLU}(W_1 \cdot \text{AvgPool}(X_i))), \quad (1)$$

where X_i is the feature map output from the i -th convolutional layer, $\text{AvgPool}(X_i)$ represents the average pooling function, W_1 and W_2 are the weight matrices of the fully connected layers, ReLU denotes the ReLU activation function [32], and σ represents the sigmoid activation function.

Next, the channel attention scores are averaged across all selected samples. The vector $\bar{s} = [\bar{s}_1, \bar{s}_2, \dots, \bar{s}_C]$ captures the general importance of each channel across the dataset.

Finally, we combine these channel attention scores \bar{s}_k with the scaling factor γ_k from the Batch Normalization (BN) layer, which inherently reflects the relative importance of the

TABLE I
COMPARISON OF PRUNING METHODS ON EUROSAT AND UCM DATASETS USING RESNET18 AND VGG16 MODELS.

Model	Method	EuroSAT			UCM			Parameters
		Acc	$\pm\Delta$	MACs	Acc	$\pm\Delta$	MACs	
ResNet18	baseline	0.870	-	0.15 G	0.849	-	2.38 G	11.18 M
	BN [33]	0.870	0		0.830	-0.019		
	L1-norm [34]	0.872	+0.002		0.833	-0.016		
	FPGM [35]	0.882	+0.012	0.02 G	0.838	-0.011	0.24 G	1.00 M
	DepGraph [14]	0.882	+0.012		0.830	-0.019		
	Ours	0.922	+0.052		0.853	+0.004		
VGG16	baseline	0.957	-	1.38 G	0.903	-	20.24 G	134.31M
	BN [33]	0.954	-0.003		0.861	-0.042		
	L1-norm [34]	0.955	-0.002		0.848	-0.055		
	FPGM [35]	0.955	-0.002	0.16 G	0.857	-0.046	1.87 G	48.90 M
	DepGraph [14]	0.953	-0.004		0.862	-0.041		
	Ours	0.957	0		0.872	-0.031		

channels in the network. The final channel importance score I_k for k -th channel in i -th layer is computed as:

$$I_{i,k} = \bar{s}_{i,k} \cdot \gamma_{i,k}. \quad (2)$$

Channels with higher $I_{i,k}$ values are considered more important during the pruning process, while channels with lower scores are pruned. For a pruning rate of α and a convolutional layer C , the pruning process can be expressed as:

$$P(C) = \{c_i \in C \mid I(c_i) \leq Q_\alpha(I(C))\}, \quad (3)$$

Where c_i is the i -th channel within C , and $I(c_i)$ denotes the importance score of channel c_i . The term $Quantile_\alpha(I(C))$ refers to the value below which the importance scores of α proportion of channels in C fall.

At this stage, the model’s original inter-layer relationships have been disrupted, leading to a significant drop in accuracy. Fine-tuning the model is necessary to restore its accuracy as closely as possible to the original level.

B. Adaptive Mining Loss

After pruning, the model’s feature extraction capability significantly diminishes due to the reduced number of parameters, leading to prediction failures on difficult samples. To address this issue, we propose an Adaptive Mining Loss (AML) function for the fine-tuning process of the pruned model.

Considering that the decline in feature extraction capability has a smaller impact on simpler samples, we can focus the fine-tuning process on learning difficult samples to compensate for the accuracy loss caused by pruning. In other words, we aim to give greater influence to the loss function from difficult samples that are predicted incorrectly. The AML function can be expressed as:

$$\mathcal{L}_{AM}(y, \hat{y}) = r \cdot \mathcal{L}_{CE}(y, \hat{y}) + e^{\frac{|y-\hat{y}|}{N} + (\frac{|y-\hat{y}|}{N})^2}, \quad (4)$$

where y is the true target value, \hat{y} is the predicted value, θ represents the parameters of the classification model, \mathcal{L}_{CE} is the cross-entropy loss, r is weight for \mathcal{L}_{CE} term in the loss function, and N is the total number of classes in the classification dataset.

To provide a more intuitive understanding of the exponential function’s impact and our loss function, we plot the loss curve

of \mathcal{L}_{LI} and its derivative with respect to a certain pixel of the model prediction \hat{y} across different prediction errors d in Fig. 2, comparing it with Cross-Entropy and Focal Loss [36].

Through the adaptive selection of difficult samples, we address the shortcomings in feature extraction capabilities of the pruned lightweight model during fine-tuning. Additionally, due to the changes in the target loss function, our method can unlock the potential of the pruned model, potentially exceeding the accuracy of the original model.

III. EXPERIMENTS

A. Datasets and Evaluation Metrics

To verify the effectiveness of our proposed approach, we adopted EuroSAT [37] and UC Merced Land-Use (UCM) [38] for experiments. EuroSAT consists of 27,000 satellite images, covering 10 different land use classes. UCM is a high-resolution remote sensing image dataset, comprising 2,100 images across 21 categories. Follow the previous work [14], [39], we utilized the Accuracy (Acc), Multiply-Accumulate Operations (MACs) and Parameters as the evaluation metrics on model performance.

B. Experimental Setup

We adopted ResNet18 [31] and VGG16 [40] as the baseline models. Except for the experiments validating the pruning rate, all other pruning rates were set to 0.7. All experiments were conducted in PyTorch with an NVIDIA RTX 3090 GPU. During the fine-tuning phase, ResNet18 employed a batch size of 64 for 40 epochs, and VGG16 deployed a batch size of 16

TABLE II
EFFECTIVENESS ANALYSIS OF CAP AND AML ON EUROSAT.

Datasets	Model	CAP	AML	Acc
EuroSAT	ResNet18			0.870
		✓	✓	0.872
		✓	✓	0.921
	VGG16			0.954
		✓	✓	0.956
		✓	✓	0.957

TABLE III
COMPARISON OF DIFFERENT LOSS FUNCTIONS ON EUROSAT.

ResNet18		VGG16	
Loss	Acc	Loss	Acc
CrossEntropy	0.917	CrossEntropy	0.956
Focal_Loss ($\gamma=1$) [36]	0.914	Focal_Loss ($\gamma=1$) [36]	0.944
Focal_Loss ($\gamma=2$) [36]	0.904	Focal_Loss ($\gamma=2$) [36]	0.933
Ours	0.921	Ours	0.957

TABLE IV
PARAMETER ANALYSIS OF BALANCE FACTOR ON EUROSAT.

Model	Results				
	r	0.1	0.4	0.7	1.0
ResNet18	r	0.1	0.4	0.7	1.0
	Acc	0.914	0.922	0.918	0.915
VGG16	r	0.1	0.4	0.7	1.0
	Acc	0.951	0.957	0.955	0.956

for 20 epochs. All models were trained leveraging an SGD optimizer [41]. The learning rate was initialized at 0.001 and adjusted employing an exponential decay method, with decay factors of 0.9 applied at 50% and 75% of the total epochs.

C. Experimental Results and Analyses

To explore the superiority of our pruning approach, we conducted comparative experiments with previous SoTA pruning methods on ResNet18 and VGG16. As shown in Tab. I, our method achieved SoTA performance on both the EuroSAT and UCM datasets. For example, on the EuroSAT dataset, ResNet18 achieved an accuracy that was 4.0% higher than the previous SoTA method DepGraph, with a 5.2% improvement over the pre-pruning model. On the UCM dataset, ResNet18 outperformed the SoTA method FPGM by 1.5% and improved by 0.4% compared to the pre-pruning model. The remarkable improvements reveal the effectiveness of our approach.

D. Ablation Studies

In this section, we validated the effectiveness of each module (CAP and AML), compared the performance of different loss functions, examined the impact of different attention mechanisms, conducted ablation on different pruning rates, and analyzed the influence of balance factors.

1) *Effectiveness of the Pruning and Fine-tuning Strategies:* We investigated the effectiveness of our proposed CAP and LIL components, as illustrated in Tab. II. By employing CAP, the accuracy improved by 4.7% on ResNet18 and by 0.2% on VGG16. The performance can be attributed to amplifying the differences in importance of model channels. After adopting AML, the accuracy further increased on two models. The experimental results demonstrate that both CAP and AML are effective and contribute to the final performance.

2) *Comparison of Different Loss Functions:* We compared our AML with various other similar loss functions like Focal loss, as represented in the Tab. III. It can be observed that both models achieved better performance during the fine-tuning phase using our AML than with Cross Entropy loss and

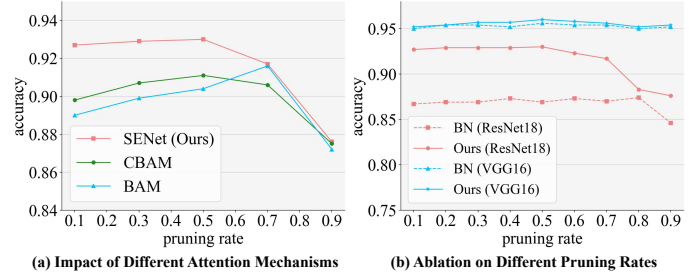


Fig. 3. Ablation studies on different attention mechanisms (a) and pruning rates (b) on EuroSAT dataset. Our approach achieved the best accuracy across all pruning rates.

different parameter settings of Focal loss. This result may be due to our loss function’s ability to better adaptively identify difficult samples and emphasize learning from them.

3) *Impact of Different Attention Mechanisms:* We investigated the influence of different attention spaces in our CAP module in Fig. 3 (a). It can be observed that SENet significantly outperformed other attention mechanisms at various pruning rates. The results indicate that channel attention is more conducive to amplifying the importance differences between channels. However, due to consideration of spatial characteristics, other types of attention mechanisms [42], [43] are not conducive to channel discrimination.

4) *Ablation on Different Pruning Rates on EuroSAT:* We conducted experiments with varying pruning rates on the EuroSAT dataset utilizing ResNet18 and VGG16, as illustrated in Tab. IV. It can be observed that our method demonstrates strong performance at various pruning rates for both models. Notably, there is a significant decline in accuracy for the ResNet18 model when the pruning rate reaches 0.9. This is due to the smaller scale of ResNet18, where a pruning rate of 0.9 results in too few model parameters, leading to a decrease in accuracy.

5) *Parameter Analysis of Balance Factors:* To ascertain the optimal balance factor value for r in the adaptive mining loss function, we conducted parameter analysis on EuroSAT dataset with ResNet18 and VGG16 as the base model. The results are illustrated in Tab IV. When r is set to 0.4, the model achieved the optimal accuracy of 92.2%. Therefore, we ultimately adopted this set of values in our method.

IV. CONCLUSION

In this paper, we proposed a high-precision model pruning algorithm, specifically designed for remote sensing image classification, which integrates channel attention mechanisms in the pruning phase with adaptive training in the fine-tuning phase. In the pruning stage, SENet architecture was utilized to map channel features into an attention space, which contributes to the precise differentiation of channel importance. Regarding the fine-tuning stage, we introduced an adaptive mining loss function that guides models to focus on difficult samples. Experimental results demonstrated the integration of these two components ensures that the model maintains high accuracy even after significant pruning.

REFERENCES

- [1] Y. Yan, Z. He, G. Liu, Y. Wang, and C. Han, "The national environmental and geological information system for remote sensing survey and monitoring," in *2015 IEEE International Geoscience and Remote Sensing Symposium (IGARSS)*. IEEE, 2015, pp. 4700–4703.
- [2] T. K. Westberry, G. M. Silsbe, and M. J. Behrenfeld, "Gross and net primary production in the global ocean: An ocean color remote sensing perspective," *Earth-Science Reviews*, vol. 237, p. 104322, 2023.
- [3] J. Wang, J. Zhen, W. Hu, S. Chen, I. Lizaga, M. Zeraatpisheh, and X. Yang, "Remote sensing of soil degradation: Progress and perspective," *International Soil and Water Conservation Research*, vol. 11, no. 3, pp. 429–454, 2023.
- [4] W. Han, X. Zhang, Y. Wang, L. Wang, X. Huang, J. Li, S. Wang, W. Chen, X. Li, R. Feng *et al.*, "A survey of machine learning and deep learning in remote sensing of geological environment: Challenges, advances, and opportunities," *ISPRS Journal of Photogrammetry and Remote Sensing*, vol. 202, pp. 87–113, 2023.
- [5] Y. An, Y. Wang, C. Liu, X. Zhang, S. Liu, and L. Du, "Geological survey of urban roadbeds utilizing rapid detection system based on transient electromagnetic method," *IEEE Transactions on Geoscience and Remote Sensing*, 2024.
- [6] Q. Zhu, X. Sun, Y. Zhong, and L. Zhang, "High-resolution remote sensing image scene understanding: A review," in *IGARSS 2019-2019 IEEE International Geoscience and Remote Sensing Symposium*. IEEE, 2019, pp. 3061–3064.
- [7] M. Mehmood, A. Shahzad, B. Zafar, A. Shabbir, and N. Ali, "Remote sensing image classification: A comprehensive review and applications," *Mathematical Problems in Engineering*, vol. 2022, no. 1, p. 5880959, 2022.
- [8] Y. Zhang, J. Liu, and W. Shen, "A review of ensemble learning algorithms used in remote sensing applications," *Applied Sciences*, vol. 12, no. 17, p. 8654, 2022.
- [9] Y. Ma, S. Chen, S. Ermon, and D. B. Lobell, "Transfer learning in environmental remote sensing," *Remote Sensing of Environment*, vol. 301, p. 113924, 2024.
- [10] S. Han, J. Pool, J. Tran, and W. Dally, "Learning both weights and connections for efficient neural network," *Advances in neural information processing systems*, vol. 28, 2015.
- [11] G. Hinton, O. Vinyals, and J. Dean, "Distilling the knowledge in a neural network," *arXiv preprint arXiv:1503.02531*, 2015.
- [12] S. Han, H. Mao, and W. J. Dally, "Deep compression: Compressing deep neural networks with pruning, trained quantization and Huffman coding," *arXiv preprint arXiv:1510.00149*, 2015.
- [13] D. Filters' Importance, "Pruning filters for efficient convnets," 2016.
- [14] G. Fang, X. Ma, M. Song, M. B. Mi, and X. Wang, "Depgraph: Towards any structural pruning," in *Proceedings of the IEEE/CVF conference on computer vision and pattern recognition*, 2023, pp. 16 091–16 101.
- [15] K. Li, G. Wan, G. Cheng, L. Meng, and J. Han, "Object detection in optical remote sensing images: A survey and a new benchmark," *ISPRS journal of photogrammetry and remote sensing*, vol. 159, pp. 296–307, 2020.
- [16] E. Maggiori, Y. Tarabalka, G. Charpiat, and P. Alliez, "Convolutional neural networks for large-scale remote-sensing image classification," *IEEE Transactions on geoscience and remote sensing*, vol. 55, no. 2, pp. 645–657, 2016.
- [17] R. Mahabir, A. Croitoru, A. T. Crooks, P. Agouris, and A. Stefanidis, "A critical review of high and very high-resolution remote sensing approaches for detecting and mapping slums: Trends, challenges and emerging opportunities," *Urban Science*, vol. 2, no. 1, p. 8, 2018.
- [18] C. Zhang, Y. Chen, X. Yang, S. Gao, F. Li, A. Kong, D. Zu, and L. Sun, "Improved remote sensing image classification based on multi-scale feature fusion," *Remote Sensing*, vol. 12, no. 2, p. 213, 2020.
- [19] C. Zhang, G. Li, and S. Du, "Multi-scale dense networks for hyperspectral remote sensing image classification," *IEEE Transactions on Geoscience and Remote Sensing*, vol. 57, no. 11, pp. 9201–9222, 2019.
- [20] S. Zhang, G. Wu, J. Gu, and J. Han, "Pruning convolutional neural networks with an attention mechanism for remote sensing image classification," *Electronics*, vol. 9, no. 8, p. 1209, 2020.
- [21] X. Wei, N. Zhang, W. Liu, and H. Chen, "Nas-based cnn channel pruning for remote sensing scene classification," *IEEE Geoscience and Remote Sensing Letters*, vol. 19, pp. 1–5, 2022.
- [22] Z. Hu, M. Gong, Y. Lu, J. Li, Y. Zhao, and M. Zhang, "Data customization-based multiobjective optimization pruning framework for remote sensing scene classification," *IEEE Transactions on Geoscience and Remote Sensing*, 2023.
- [23] L. Pham, C. Le, D. Ngo, A. Nguyen, J. Lampert, A. Schindler, and I. McLoughlin, "A light-weight deep learning model for remote sensing image classification," in *2023 International Symposium on Image and Signal Processing and Analysis (ISPA)*. IEEE, 2023, pp. 1–6.
- [24] Z. Chen, J. Yang, Z. Feng, and L. Chen, "Rscnet: An efficient remote sensing scene classification model based on lightweight convolution neural networks," *Electronics*, vol. 11, no. 22, p. 3727, 2022.
- [25] Z. Li, H. Shen, Q. Weng, Y. Zhang, P. Dou, and L. Zhang, "Cloud and cloud shadow detection for optical satellite imagery: Features, algorithms, validation, and prospects," *ISPRS Journal of Photogrammetry and Remote Sensing*, vol. 188, pp. 89–108, 2022.
- [26] N. Gulat and A. Kaushik, "Remote sensing image restoration using various techniques: A review," *International Journal of Scientific & Engineering Research*, vol. 3, no. 1, p. 6, 2012.
- [27] B.-C. Gao, M. J. Montes, C. O. Davis, and A. F. Goetz, "Atmospheric correction algorithms for hyperspectral remote sensing data of land and ocean," *Remote sensing of environment*, vol. 113, pp. S17–S24, 2009.
- [28] H. Hosseini and M. Khoshsima, "Comprehensive investigation of the atmospheric modulation transfer function (mtf) for satellite imaging payloads: considering turbulence and aerosol effects over tehran," *Physica Scripta*, vol. 99, no. 7, p. 075044, 2024.
- [29] M. Hassanin, S. Anwar, I. Radwan, F. S. Khan, and A. Mian, "Visual attention methods in deep learning: An in-depth survey," *Information Fusion*, vol. 108, p. 102417, 2024.
- [30] J. Hu, L. Shen, and G. Sun, "Squeeze-and-excitation networks," in *Proceedings of the IEEE conference on computer vision and pattern recognition*, 2018, pp. 7132–7141.
- [31] K. He, X. Zhang, S. Ren, and J. Sun, "Deep residual learning for image recognition," in *Proceedings of the IEEE conference on computer vision and pattern recognition*, 2016, pp. 770–778.
- [32] X. Glorot, A. Bordes, and Y. Bengio, "Deep sparse rectifier neural networks," in *Proceedings of the fourteenth international conference on artificial intelligence and statistics*. JMLR Workshop and Conference Proceedings, 2011, pp. 315–323.
- [33] Z. Liu, J. Li, Z. Shen, G. Huang, S. Yan, and C. Zhang, "Learning efficient convolutional networks through network slimming," in *Proceedings of the IEEE international conference on computer vision*, 2017, pp. 2736–2744.
- [34] H. Li, A. Kadav, I. Durdanovic, H. Samet, and H. P. Graf, "Pruning filters for efficient convnets," *arXiv preprint arXiv:1608.08710*, 2016.
- [35] Y. He, P. Liu, Z. Wang, Z. Hu, and Y. Yang, "Filter pruning via geometric median for deep convolutional neural networks acceleration," in *Proceedings of the IEEE/CVF conference on computer vision and pattern recognition*, 2019, pp. 4340–4349.
- [36] T.-Y. Lin, P. Goyal, R. Girshick, K. He, and P. Dollár, "Focal loss for dense object detection," in *Proceedings of the IEEE international conference on computer vision*, 2017, pp. 2980–2988.
- [37] P. Helber, B. Bischke, A. Dengel, and D. Borth, "Eurosat: A novel dataset and deep learning benchmark for land use and land cover classification," *IEEE Journal of Selected Topics in Applied Earth Observations and Remote Sensing*, 2019.
- [38] B. Qu, X. Li, D. Tao, and X. Lu, "Deep semantic understanding of high resolution remote sensing image," in *2016 International conference on computer, information and telecommunication systems (Cits)*. IEEE, 2016, pp. 1–5.
- [39] Y. Wang, S. Guo, J. Guo, J. Zhang, W. Zhang, C. Yan, and Y. Zhang, "Towards performance-maximizing neural network pruning via global channel attention," *Neural Networks*, vol. 171, pp. 104–113, 2024.
- [40] K. Simonyan and A. Zisserman, "Very deep convolutional networks for large-scale image recognition," *arXiv preprint arXiv:1409.1556*, 2014.
- [41] J. M. Cherry, C. Adler, C. Ball, S. A. Chervitz, S. S. Dwight, E. T. Hester, Y. Jia, G. Juvik, T. Roe, M. Schroeder *et al.*, "Sgd: Saccharomyces genome database," *Nucleic acids research*, vol. 26, no. 1, pp. 73–79, 1998.
- [42] S. Woo, J. Park, J.-Y. Lee, and I. S. Kweon, "Cbam: Convolutional block attention module," in *Proceedings of the European conference on computer vision (ECCV)*, 2018, pp. 3–19.
- [43] J. Park, "Bam: Bottleneck attention module," *arXiv preprint arXiv:1807.06514*, 2018.